On the Need of Intermediate Complexity General Circulation Models

A "SPEEDY" Example

BY FRED KUCHARSKI, FRANCO MOLTENI, MARTIN P. KING, RICCARDO FARNETI, IN-SIK KANG, AND LAURA FEUDALE

The use of idealized climate models in the search for physical understanding of the behavior of complex general circulation models (GCM) has been advocated before by Held, Nof, Colin de Verdiere, and others, but the use of a hierarchy of models to test a scientific question or physical phenomena is receiving little attention in the climate community. The expression "hierarchy" is used in a quite generic sense, from analytical models of single physical systems, such as the Madden–Julian oscillation, for example, to state-of-the-art GCM simulations. There are many examples of the use of a hierarchy of models in climate variability studies, and we mention here two classical examples. The first is the delayed oscillator model constructed to investigate ENSO variability that is still being used in the interpretation of the results from complex coupled models. The second example is the use of simple coupled models of air–sea interaction to understand midlatitude SST feedbacks on the atmospheric circulation in complex models.

Another class in the hierarchy of models has an intermediate complexity representation of physical processes that allows realistic and fast climate simulations that often involve large ensembles for the purpose of reducing uncertainty and estimation of the forced and internal variability of the system. The forced signal is typically estimated by an ensemble mean of many simulations, but ensembles of state-of-the-art models are often too small to reduce the remaining internal variability. The ensemble size needed to estimate the mean accurately depends on the signal-to-noise ratio for the variable and region under consideration. For example, the ensemble size to estimate midlatitude 500-hPa height accurately is about 20, which is larger than most ensembles used in seasonal hindcast datasets or climate projections performed by individual centers. Intermediate complexity models can also be used efficiently to investigate the sensitivity of simulated climate to changes in parameters in the physical parameterizations. Another application is related to climate change. For example, Forest et al. (2002) and Sokolov at al. (2009) use the MIT Integrated Global System Model (MIT IGSM) to investigate topics such as climate sensitivity, aerosol forcing, ocean heat uptake rate, and probabilistic projections of climate change. There are many intermediate complexity models, some of which have been developed into Earth system models of intermediate complexity (EMICs). A number of them are participating in the IPCC Fifth Assessment Report and can be found at http://climate.uvic.ca/EMICAR5 (one of which is based on a previous version of the model introduced here). This website also provides information about experiments that are performed with these models that range from ensembles of 1,000-year-long historical simulations to the assessment of different CO_2 concentration pathways.

Here, we reemphasize the importance of intermediate complexity modeling and suggest that results from such a model are useful in the understanding of climate variability and change.

AFFILIATIONS: KUCHARSKI AND FARNETI—The Abdus Salam International Centre for Theoretical Physics, Earth System Physics Section, Trieste, Italy; MOLTENI—European Centre For Medium-Range Weather Forecasts, Berkshire, Reading, United Kingdom; KING—Bjerknes Centre for Climate Research, Uni Research, Bergen, Norway; KANG—Seoul National University, Seoul, South Korea; FEUDALE—OSMER Osservatorio Meteorologico Regionale dell'ARPA Friuli Venezia Giulia, Visco, Italy
CORRESPONDING AUTHOR: Fred Kucharski, The Abdus Salam International Centre for Theoretical Physics, Earth System Physics Section, Strada Costiera, 11, I-34151 Trieste, Italy
E-mail: kucharsk@ictp.it

DOI:10.1175/BAMS-D-11-00238.1

Equally important is the role of intermediate complexity models as a tool for researchers with less than optimal resources, a situation that still prevails in many developing countries.[1]

Another important area where intermediate complexity models are widely used is in the work of graduate students, who gain better scientific and software insights permitted by a simpler model than might be possible with state-of-the-art GCMs. Some more advantages of intermediate complexity models are that many of them are well documented and freely available for download and use. They are constructed in a way to facilitate the experimentation with different forcings, coupling approaches, parameterizations, etc., which encourages creativity in pursuing an understanding of the fundamental science.

An example of an intermediate complexity model is the atmospheric general circulation model (AGCM) developed at the Abdus Salam International Centre for Theoretical Physics—the ICTPAGCM, also called SPEEDY, from Simplified Parameterizations, primitivE-Equation DYnamics. The website http://users.ictp.it/~kucharsk/speedy-net.html provides descriptions of the latest and previous model versions, an assessment of the performance of the model in representing the mean climate, a list of users, and downloading information. In the latest version (41) of the model, there are 8 vertical levels, and the most commonly used horizontal spectral truncations are T30 (about 3.75° × 3 75° horizontal resolution) and T47 (about 2.5° × 2.5° horizontal resolution). The model includes physically based parameterizations of large-scale condensation, shallow and deep convection, shortwave and longwave radiation, surface fluxes of momentum, heat and moisture, and vertical diffusion. The 5-layer version of the model was originally described by Molteni in 2003, and the current 8-layer version was described by Kucharski et al. in 2006. The model is computationally inexpensive, due mainly to the simplified parameterizations, as well as the relatively low horizontal and vertical resolution adopted. For example, the boundary layer in the ICTPAGCM is represented by just one model layer, and the shortwave radiation scheme only uses two spectral bands, while four are used in the longwave radiation scheme. A few details regarding the computational efficiency are given here: using a single core on a 2.4-GHz Xeon with a 2-MB CPU cache, an ICTPAGCM built with an Intel compiler can simulate 1 year in 6 minutes (using a standard application). Thus, in one day the ICTPAGCM can simulate 240 model years. The memory requirement is about 35 MB, which can be run without difficulty even on older desktop computers of rather low hardware specifications. For comparison, on a single core, a state-of-the-art model run at similar horizontal resolution typically requires a CPU time of about one day to simulate one model year. This means that to construct large ensembles (about 100 members) of century-long simulations on a small cluster of 100 cores would take about 3 months.

The ICTPAGCM model is very flexible in the sense that it can be easily modified to address a wide range of problems. In many aspects, the ICTPAGCM achieves capability that is on par with state-of-the-art models in simulating the climatic mean and variability. This is especially true for large-scale features. In certain types of studies, the performance of state-of-the-art models can even be exceeded, because it is easy to modify the experimental set-up to optimize performance (e.g., in "pacemaker" experiments for Indian Monsoon simulations, as discussed by Kucharski et al. in a 2007 *Journal of Climate* article).

Scientific research using the ICTPAGCM in recent years covers a broad range of topics in climate variability—for example, modes of extratropical planetary-scale variability (Molteni et al. 2011); extratropical circulation trends and decadal changes (e.g., Kucharski et al. 2006); tropical–extratropical teleconnections, monsoon climate, and its variability; ENSO–monsoon relationships and their decadal changes; tropical teleconnection patterns (e.g., Kucharski et al. 2007; Kucharski et al. 2012; Barimalala et al. 2011); and ENSO teleconnection changes in global warming scenarios (e.g., Herzeg-Bulic et al. 2012). In some studies, the ICTPAGCM has been coupled to full or simplified ocean models. For a list of publications with ICTP involvement, see http://users.ictp.it/~kucharsk/speedy-doc.html. The ICTPAGCM is constantly evolving and being improved, and much effort has recently been devoted to the inclusion of new subcomponents of the climate system. In a collaborative project with the University of Maryland,

[1] This paper was motivated by the Workshop on Hierarchical Modeling of Climate (http://cdsagenda5.ictp.it/full_display.php?ida=a10154), held at the Abdus Salam International Centre for Theoretical Physics (ICTP) in Trieste, Italy, on 18–22 July 2011. The mission of ICTP is to foster research in developing countries. More than 100 researchers from developing and developed countries participated in this conference.

the ICTPAGCM coupled to the VEGAS land surface and interactive vegetation model is being tested for a future coupling to a human population model.

Here we provide two examples of applications of the latest version (41) of the ICTPAGCM. The first is the investigation of the origin of African and Indian monsoon megadroughts, a topic of particular interest for the developing countries affected by the drought. Feudale and Kucharski (2012), hereafter referred to as FK12, have identified that the Sahelian and Indian monsoon rainfall in observations and simulations with the ICTPAGCM show a common multidecadal variability with maximum values in the 1950s to early 1960s and minimum values in the 1980s to early 1990s. Figure 1 (top) shows the June–September (JJAS) rainfall change for the period 1980–94 relative to 1950–64, using the rainfall data from the Climatic Research Unit (CRU). The Sahel and Indian monsoon experienced a significant tendency toward drought conditions from the 1950–64 period to the 1980–94 period. It is important to understand the mechanisms for such changes, as extremely vulnerable societies are affected. FK12 pointed to a global SST pattern as the forcing for this Sahel/Indian megadrought phenomenon. ICTPAGCM forced with monthly-varying observed SSTs was able to reproduce the decadal temporal behavior of the observed rainfall in both monsoon regions (no other forcing has been included; for example, CO_2 is fixed at the value of 1990). Figure 1 (bottom) shows the simulated rainfall 1980–94 minus 1950–64 JJAS difference of an ensemble mean of 20 simulations with the ICTPAGCM that cover the period 1949–2008. Different ensemble members have been constructed by small perturbations in the initial conditions and a one-year spin-up period. The model reproduces the broad features of the observed changes, namely the drying in the Sahelian and Indian region, although the responses are shifted slightly to the south in both regions and are weaker in the Sahel region.

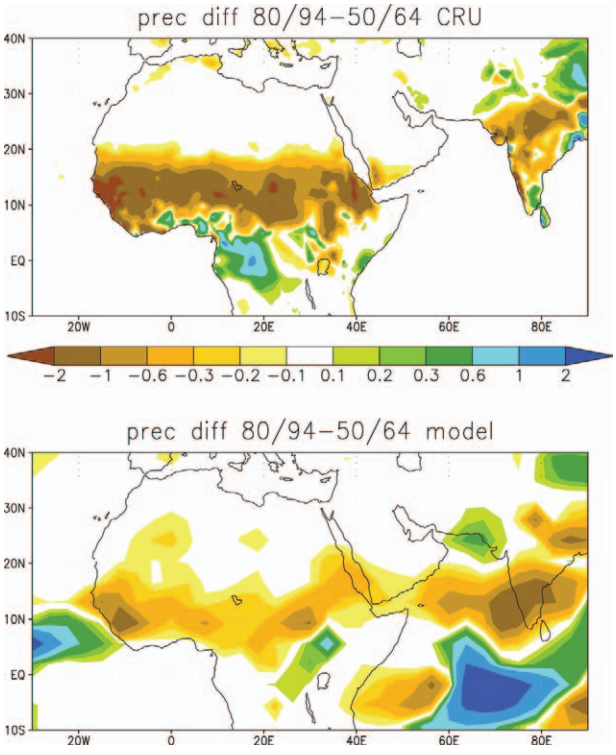

Fig. 1. JJAS rainfall difference 1980–94 minus 1950–64: (top) CRU observations; (bottom) ICTPAGCM. Units are mm day^{-1}.

The SST pattern [derived from the Hadley Centre HadISST; Rayner et al. (2003)] associated with the drought pattern is shown in Fig. 2. A strong warming appears in all tropical regions and a cooling is visible in the extratropical North Pacific and Atlantic. The Pacific/Indian Ocean SST pattern is similar to the interdecadal Pacific oscillation (IPO), whereas the northern Atlantic cooling could be related to the negative phase of the Atlantic multidecadal oscillation (AMO). Both patterns have been identified as causing Indian and Sahel droughts. Furthermore, a warm tropical Atlantic may also contribute to a drying of both monsoon systems. The combined effect of the global SST forcing shown in Fig. 2 is an upper-level high pressure in the equatorial region and, at low levels, higher pressure in the Saharan and Indian region, which is favorable for low-level divergence

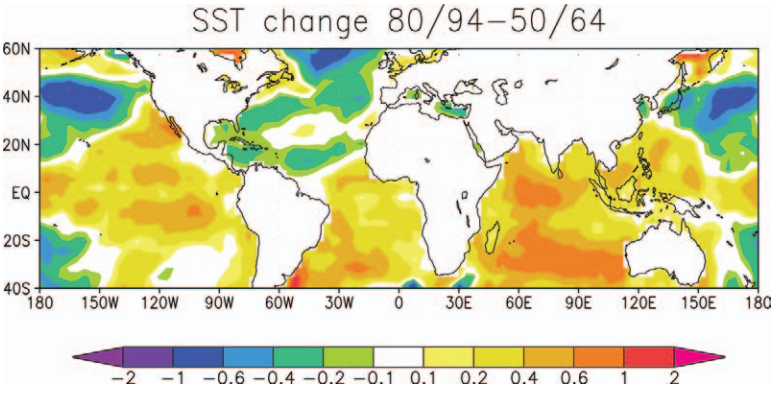

Fig. 2. JJAS sea surface temperature difference (using the Hadley Centre HadISST data) 1980–94 minus 1950–64. Units are K.

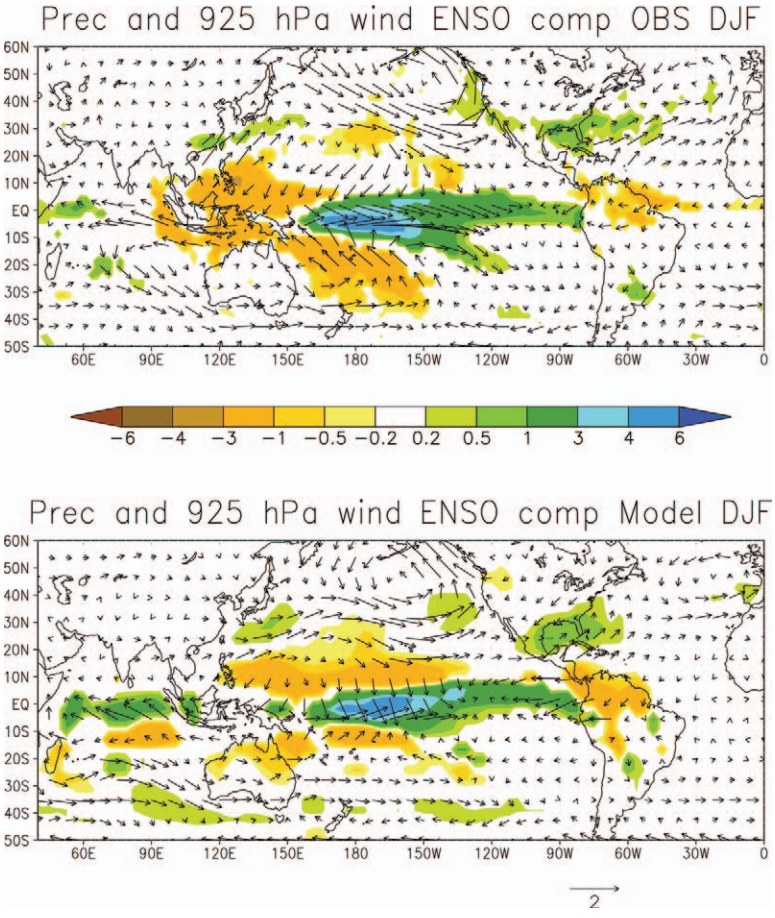

Fig. 3. Regression of anomalies of precipitation and 925-hPa winds onto the DJF Niño-3.4 index: (top) CMAP rainfall and NCEP–NCAR reanalysis winds; (bottom) ICTPAGCM. For rainfall, all anomalies shown are 95% statistically significant. Units are mm day^{-1} for rainfall and m s^{-1} for wind.

and reduced rainfall in the Sahel and Indian region. The ability of AGCMs—particularly the ones with intermediate complexity—to reproduce the decadal behavior of large parts of the Northern Hemispheric monsoon systems is encouraging and indicates a potential predictability if decadal SST variations could be predicted with sufficient skill.

The second example highlights the use of the ICTPAGCM as an educational tool and demonstrates its ability to reproduce the response to an important phenomenon in climate variability. Here, the well-documented ENSO response is analyzed by showing composites based on regression maps of several fields onto the December–February (DJF) Niño-3.4 index (here defined as the mean SST in the region 190°E to 240°E, 5°S to 5°N) for a 51-yr period (1950–2000). The regression maps are calculated from the covariance of the normalized Niño-3.4 index with the anomalies of the respective field. Figure 3 (top) shows the regression map for observed rainfall (CMAP; Xie and Arkin 1997; available only from 1979) and NCEP–NCAR reanalysis 925-hPa winds, while in Fig. 3 (bottom), the modeled counterpart is shown, using the ensemble also used in the first example. Overall, the model is able to reproduce the direct rainfall response to the ENSO forcing with increased rainfall of about 5 mm day^{-1} in the central equatorial Pacific. The direct 925-hPa wind response is also well reproduced overall with convergence and westerly anomalies also located in the central equatorial Pacific, providing the positive atmospheric feedback to the ENSO phenomenon. Interestingly, a number of teleconnected responses are also reproduced reasonably well by the model. For example, there is a drying surrounding the equatorial positive rainfall response as well as in equatorial Central America. A positive rainfall and cyclonic circulation response is seen near the California coast and Aleutian region as well as in the Gulf of Mexico and Florida region, extending further into the western Atlantic. Other features are not so well reproduced, such as the observed drying in the Indonesian Archipelago, where the model rainfall response is weak.

The model's performance in reproducing several ENSO teleconnections has been documented in the scientific literature. The aforementioned teleconnection to the Pacific/North American region can be understood as related to the extratropical wave train induced by ENSO. A way to better identify this wave train is to analyze the regression map for the 200-hPa height. Figure 4 (top) and Fig. 4 (bottom) show the 200-hPa height ENSO regression maps for observations (NCEP–NCAR reanalysis) and the model, respectively. The wave train in the observations in the northern hemisphere is clearly visible, with alternating positive and negative 200-hPa height anomalies in the Pacific

region and extending into North America. Again, this ENSO-induced wave train is well reproduced by the model, with slightly reduced amplitude in the Pacific region. We can also infer from comparing Figs. 3 and 4 that the North Pacific/North American responses are nearly barotropic (e.g., the Aleutian low is present also at 200 hPa). Extratropical rainfall responses may be explained by the position of the wave response over the region under consideration. For example, the increased rainfall close to the California coast may be explained by rising motion induced on the eastward side of the Aleutian low, whereas the rainfall increases in the Gulf of Mexico and Florida region may be explained by the rising motion induced on the southeastern side of the low pressure located over North America at about 35°N, and by the low-level convergence induced by the low itself. In tropical regions, widespread increased heights can be seen in the observations and the model. The reason is that the ENSO-induced heating is distributed effectively in the zonal direction by fast equatorial wave propagation, leading to a hydrostatically induced positive height perturbation.

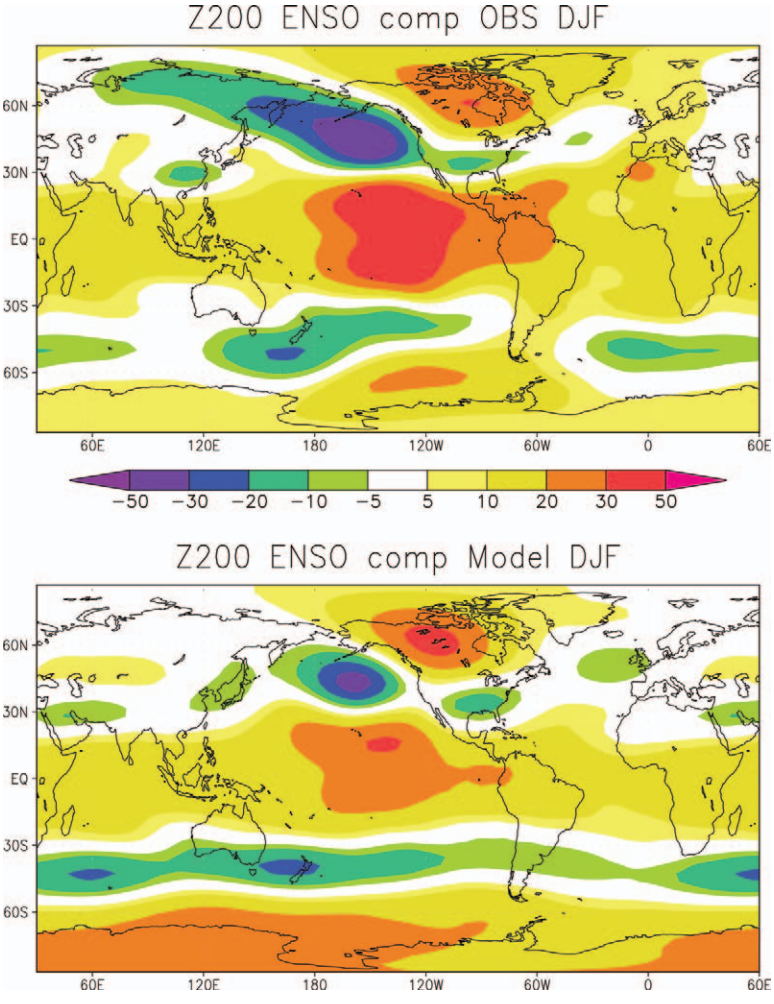

Fig. 4. Regression of anomalies of 200-hPa heights onto the DJF Niño-3.4 index: (top) NCEP–NCAR reanalysis; (bottom) ICTPAGCM. Units are m.

The Earth System Physics Section at ICTP, together with the external authors on this report, is working toward a flexible Earth-system model based on the ICTPAGCM and the modular ocean model (MOM). The aim is to provide a modeling system that can still be run on commonly used personal computers and that allows efficient investigations of a broad range of research questions arising in the field of Earth-system science. We believe that such an Earth-system model will fit well into the ensemble of already existing EMICs (e.g., listed at http://climate.uvic.ca/EMICAR5).

ACKNOWLEDGMENTS. The authors gratefully thank the editor and the three anonymous reviewers for their constructive comments and suggestions to improve the manuscript.

FOR FURTHER READING

Barimalala, R., A. Bracco, and F. Kucharski, 2011: The representation of the South Tropical Atlantic teleconnection to the Indian Ocean in the AR4 coupled models. *Climate Dyn.*, doi:10.1007/s00382-011-1082-5.

Barsugli, J. J., and D. S. Battisti, 1998: The basic effects of atmosphere–ocean thermal coupling on midlatitude variability. *J. Atmos. Sci.,* **55,** 477–493.

Bretherton, C. S., and D. S. Battisti, 2000: An interpretation of the results from atmospheric general circulation models forced by the time history of the observed sea surface temperature distribution. *Geophys. Res. Lett.,* **27,** 767–770, doi:10.1029/1999GL010910.

Colin de Verdiere, A., 2009: Keeping the freedom to build idealized climate models. *EOS Trans. AGU,* **90,** 224.

Deque, M., 1997: Ensemble size for numerical seasonal forecasts. *Tellus,* **49A,** 74–86.

Diaz, H., M. Hoerling, and J. Eischeid, 2001: ENSO variability, teleconnections and climate change. *Int. J. Climatol.,* **21,** 1845–1862.

Feudale, L., and F. Kucharski, 2012: Mechanism connecting African and Indian monsoon megadroughts. *Climate Dyn.,* submitted.

Forest, C. E., P. H. Stone, A. P. Sokolov, M. R. Allen, and M. D. Webster, 2002: Quantifying uncertainties in climate system properties with the use of recent climate observations. *Science,* **295,** 113–117, doi:10.1126/science.1064419.

Giannini, A., R. Saravanan, and P. Chang, 2003: Oceanic forcing of Sahel rainfall on interannual to interdecadal time scales. *Science,* **302,** 1027–1030.

Griffies, S. M., and Coauthors, 2005: Formulation of an ocean model for global climate simulations. *Ocean Science,* **1,** 45–79.

Held, I. M., 2005: The gap between simulation and understanding in climate modeling. *Bull. Amer. Meteor. Soc.,* doi:10.1175/BAMS-86-11-1609.

Herceg-Bulic, I., C. Brankovic, and F. Kucharski, 2012: ENSO teleconnections in a warmer climate. *Climate Dyn.,* **38,** 1593–1613, doi:10.1007/s00382-010-0987-8.

Kalnay, E., and Coauthors, 1996: The NCEP/NCAR 40-Year Reanalysis Project. *Bull. Amer. Meteor. Soc.,* **77,** 437–471.

Kucharski, F., F. Molteni, and A. Bracco, 2006: Decadal interactions between the Western Tropical Pacific and the North Atlantic Oscillation. *Climate Dyn.,* **26,** 79–91, doi:10.1007/s00382-005-0085-5.

——, A. Bracco, J. H. Yoo, and F. Molteni, 2007: Low-frequency variability of the Indian Monsoon–ENSO relation and the Tropical Atlantic: The "weakening" of the '80s and 90s. *J. Climate,* **20,** 4255–4266, doi:10.1175/JCLI4254.1.

——, and Coauthors, 2009: The CLIVAR C20C project: Skill of simulating Indian monsoon rainfall on interannual to decadal timescales. Does GHG forcing play a role? *Climate Dyn.,* **33,** 615–627, doi:10.1007/s00382-008-0462-y.

——, N. Zeng, and E. Kalnay, 2012: A further assessment of vegetation feedback on decadal Sahel rainfall variability. *Climate Dyn.,* doi:10.1007/s00382-012-1397-x.

Mitchell, T. D., and P. D. Jones, 2005: An improved method of constructing a database of monthly climate observations and associated high-resolution grids. *Int. J. Climatol.,* **25,** 693–712.

Molteni, F., 2003: Atmospheric simulations using a gcm with simplified physical parametrizations. I: Model climatology and variability in multi-decadal experiments. *Climate Dyn.,* **20,** 175–191.

——, M. P. King, F. Kucharski, and D. M. Straus, 2011: Planetary-scale variability in the northern winter and the impact of land–sea thermal contrast. *Climate Dyn.,* **37,** 151–170, doi:10.1007/s00382-010-0906-z.

Neelin, D., A. Bracco, H. Luo, J. C. McWilliams, and J. E. Meyerson, 2010: Considerations for parameter optimization and sensitivity in climate models. *Proc. Natl. Acad. Sci.,* doi:10.1073/pnas.1015473107.

Nof, D., 2008: Simple versus complex climate modeling. *EOS Trans. AGU,* **89,** 544–545.

Rayner, N. A., D. E. Parker, E. B. Horton, C. K. Folland, L. V. Alexander, D. P. Rowell, E. C. Kent, and A. Kaplan, 2003: Global analyses of sea surface temperature, sea ice, and night marine air temperature since the late nineteenth century. *J. Geophys. Res.,* **108,** doi:10.1029/2002JD002670.

Sokolov, A. P., P. H. Stone, C. E. Forest, R. Prinn, M. C. Sarofim, M. Webster, S. Paltsev, and C. A. Schlosser, 2009: Probabilistic forecast for twenty-first-century climate based on uncertainties in emissions (without policy) and climate parameters. *J. Climate,* **32,** 5175–5204.

Suarez, M. J., and P. S. Schopf, 1988: A delayed action oscillator for ENSO. *J. Atmos. Sci.,* **45,** 3283–3287.

Xi, P., and P. A. Arkin, 1997: Global precipitation: A 17-year monthly analysis based on gauge observations, satellite estimates and numerical model outputs. *Bull. Amer. Meteor. Soc.,* **78,** 2539–2558.

Zeng, N., J. D. Neelin, K.-M. Lau, and C. J. Tucker, 1999: Enhancement of interdecadal climate variability in the Sahel by vegetation interaction. *Science,* **286,** 1537–1540.